

Growth, Structural, Spectral And Electrical Studies Of Semi Organic Amino-Nitrate (GPC) Crystal

Shailesh S Dongare

Department Of Physics, S. G. Arts, Science And G. P. Commerce College, Shivle, Murbad-421401, India

Abstract:

The advancement of photonics and optoelectronic technologies relies significantly on the development of high-performance materials with excellent nonlinear optical (NLO) properties. Semi-organic compounds, particularly those formed by the combination of amino acids and inorganic salts, have emerged as promising candidates for second harmonic generation (SHG) due to their favorable optical and mechanical characteristics. In this study, a novel semi-organic amino-nitrate crystal glycine-potassium-calcium nitrate (GPC) was successfully synthesized and evaluated for its NLO potential. GPC crystals were grown at ambient temperature using the slow evaporation technique from an aqueous solution, yielding transparent crystals of dimensions $11 \times 9 \times 5 \text{ mm}^3$ within 3-4 weeks. The solubility of GPC in water was measured, and the crystal structure was determined to be orthorhombic with lattice parameters $a = 21.2907 \text{ \AA}$, $b = 7.7940 \text{ \AA}$, $c = 6.5552 \text{ \AA}$, and a unit cell volume of 1082.77 \AA^3 . Elemental composition was confirmed using CHN analysis, EDAX, and NMR spectroscopy. Comparative IR and Raman studies suggest the absence of a center of symmetry, a desirable trait for NLO materials. UV-visible spectroscopy reveals a broad transparency window suitable for optoelectronic applications. The SHG efficiency of GPC, measured using a Nd:YAG laser (1064 nm), was found to be 0.45 times that of standard potassium dihydrogen phosphate (KDP). Additional studies, including photoconductivity and I-V characterization, further support the potential of GPC crystals in nonlinear optical applications.

Key Word: - Crystal growth, XRD, NMR, FTIR, RAMAN SHG.

Date of Submission: 19-05-2025

Date of Acceptance: 29-05-2025

I. Introduction

Remarkable advancements in optical technologies have been propelled by the development of innovative materials capable of strong light-matter interactions. Among the most promising of these are semi-organic compounds, which have recently garnered significant interest due to their potential in second harmonic generation (SHG) a pivotal nonlinear optical (NLO) phenomenon. Notably, complexes formed by amino acids in combination with various ionic salts have demonstrated favorable properties for NLO applications [1,2]. The amino acid α -glycine is frequently utilized in the synthesis of both organic and semi-organic materials because of its ability to exhibit diverse functional characteristics, including dielectric, ferroelectric, nonlinear optical behavior, and light sensitivity [3,4]. However, purely organic NLO materials often suffer from limitations such as reduced thermal and mechanical stability. This drawback stems from their molecular structure, which typically features relatively large interatomic distances and weak intermolecular forces. The incorporation of inorganic components into the organic matrix has proven effective in improving these properties, enhancing both mechanical durability and thermal stability, thereby making such hybrid materials more viable for practical photonic applications.

Hybrid semi-organic materials are currently being explored for use in a wide array of applications, including optical switching, frequency conversion, and image processing. These materials benefit from the high NLO efficiency intrinsic to organic molecules, along with the structural reinforcement offered by inorganic constituents. Various amino acids, such as glycine, L-arginine, and L-histidine have been investigated in combination with different metal salts to create functional crystalline materials with promising optical properties [5,6]. Glycine, in particular, is known to crystallize in three polymorphic forms: α , β , and γ , with the α -form being the most stable and widely studied. Several studies have explored the combination of α -glycine with nitrates such as sodium nitrate (NaNO_3) [7], silver nitrate (AgNO_3) [8], and calcium nitrate [$\text{Ca}(\text{NO}_3)_2$] [9], producing new materials with appreciable NLO activity. For instance, in glycine sodium nitrate crystals, the glycine retains its zwitterionic form while sodium ions adopt an eightfold coordination, resulting in a distorted hexagonal bipyramidal geometry. The glycine molecules engage in head-to-tail hydrogen bonding, forming layered arrangements that facilitate intermolecular interactions critical for nonlinear optical behavior [10]. This structural adaptability of α -glycine makes it an excellent candidate for crystal engineering involving both organic and inorganic species.

In the present investigation, a novel semi-organic glycine potassium-calcium nitrate (GPC) crystals were grown from aqueous solution via slow evaporation at ambient temperature. Their structure and composition were examined using CHN elemental analysis, energy dispersive X-ray analysis (EDAX), X-ray diffraction (XRD), Fourier transform infrared spectroscopy (FTIR), UV-visible spectroscopy, and SHG studies. Electrical properties were evaluated through I-V characteristics to further assess the material's potential for optoelectronic applications.

II. Growth And Solubility

Semi-organic glycine mixed nitrate (GPC) crystal were synthesized using analytical AR grade α -glycine, Potassium nitrate $[KNO_3]$ and Calcium nitrate $[Ca(NO_3)_2]$ in molar ratio 3:0.5:0.5. The precursor materials were dissolved in double-distilled water, and the initial pH of the solution was maintained at 5.8. The crystals were grown using the slow evaporation technique from an aqueous solution under ambient conditions. After a growth period of approximately three to four weeks, transparent crystals of size $(11 \times 9 \times 5 \text{ mm}^3)$ were obtained in about 3-4 weeks at room temperature (Fig. 1). The size of the grown crystals was found to be dependent on the availability of solute in the solution, which is primarily governed by the solubility of the material in the solvent. The solubility of GPC crystals was determined in distilled water at four different temperatures using a constant temperature bath (Fig. 2). The results indicate that solubility increases with temperature, following a nearly linear trend in the range of 300 K to 350 K.

The density of GPC crystals was measured using the flotation method, yielding a recorded value of 1.612 g/cc. Thermal analysis revealed that the melting point of GPC crystals is 216 °C, while decomposition occurs at 235 °C, indicating the thermal stability of the material under moderate heating conditions.

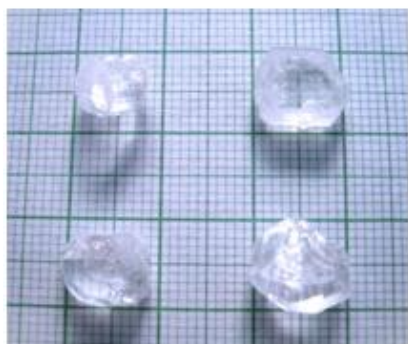


Figure.1 As grown GPC crystal.

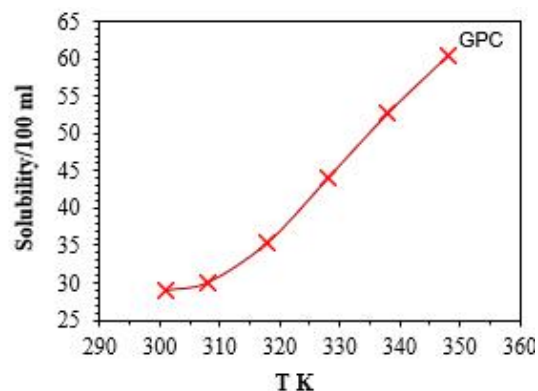


Figure.2 Solubility curve for GPC crystal

III. CHN And EDAX Analysis

The elemental composition of the grown GPC crystal was analyzed using a CHN analyzer (THERMO FINIGAN FLASH 1112 SERIES) and an energy dispersive X-ray analysis (EDAX) system attached to a scanning electron microscope (JSM-840). These techniques provide crucial information about the presence of organic and inorganic elements in the crystal, ensuring its chemical integrity and confirming its stoichiometry. CHN analysis was employed to determine the percentage of carbon (C), hydrogen (H), and nitrogen (N) in the GPC crystal. This method is essential for validating the presence of organic components in the crystal lattice. The obtained data (Table 1) reveal that nitrogen, carbon, and hydrogen are present at significant levels, which aligns with the expected composition of the synthesized GPC crystal. The CHN spectrum (Figure 3) further confirms these findings, highlighting the presence of these elements in the molecular framework.

The oxygen content was estimated by considering the total composition of the sample as 100% and subtracting the measured CHN values, along with other inorganic elements identified through EDAX. This approach allows for an indirect quantification of oxygen, which plays a critical role in the stability of the crystal lattice and its interaction with other elements. EDAX was performed to identify and quantify inorganic elements present in the crystal. The results indicate the presence of potassium (K) and calcium (Ca), which correspond to the expected chemical composition of the crystal, namely $(KNO_3)_{1/2} \cdot (NH_2CH_2COOH)_3 \cdot (Ca(NO_3)_2)_{1/2}$. The elemental peaks observed in the EDAX spectrum confirm the incorporation of these elements into the crystal matrix.

The retention times for different peaks were recorded at 0.8 min, 1.24 min, and 3.55 min, correlating with the elemental components identified (Table 1). The obtained elemental percentages 17.655% nitrogen,

23.685% carbon, and 4.922% hydrogen are consistent with the theoretical composition of the crystal, confirming the successful synthesis of the GPC crystal with the expected stoichiometric balance. In the GPC sample presence of carbon, hydrogen and nitrogen were traced in percentages shown in CHN spectrum (Figure 3). The combined CHN and EDAX analyses validate the structural integrity and elemental composition of the GPC crystal. The presence of both organic and inorganic components suggests a stable molecular framework suitable for further characterization and potential applications in optical, electronic, or structural studies. The agreement between experimental and theoretical compositions underscores the reliability of the synthesis method and the purity of the obtained crystal.

Table 1 Elemental analysis of GPC crystal.

Sample-GPC	%N	%C	%H	%O	%EDAX Element	Chemical Unit
Peak No.	1	2	3	53.738	K, Ca	$(\text{KNO}_3)_{1/2}(\text{NH}_2\text{CH}_2\text{COOH})_3(\text{Ca}(\text{NO}_3)_2)_{1/2}$
Retention time	0.8	1.24	3.55			
Elements (%)	17.655	23.685	4.922			

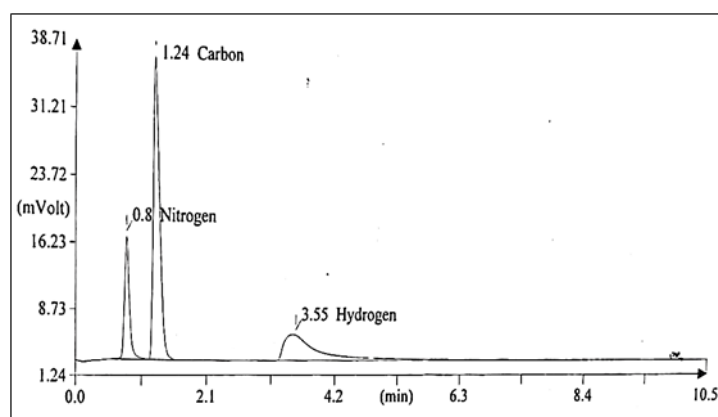


Figure. 3 CHN spectrum for GPC crystal.

IV. X-Ray Diffraction Studies

To confirm the crystalline phase and structural characteristics of the synthesized glycine potassium-calcium nitrate (GPC) crystal, X-ray powder diffraction (XRD) analysis was carried out using a JEOL X-ray diffractometer system (JDX-8030 Series) with Cu-K α radiation ($\lambda = 1.541 \text{ \AA}$). The diffraction pattern was recorded over a 2θ range of 10° to 80° , with a scanning rate of 5° per minute [11,12]. The diffraction data were analyzed using POWD—an interactive powder diffraction data interpretation and indexing software (Version 2.2, Australia). The observed diffraction peaks were indexed, and the results confirmed that the GPC crystal crystallizes in the orthorhombic system with calculated lattice parameters: $a = 21.2907 \text{ \AA}$, $b = 7.7940 \text{ \AA}$, $c = 6.5552 \text{ \AA}$, yielding a unit cell volume of 1082.77 \AA^3 . A set of intense diffraction peaks was observed in the range 20° – 30° , with the maximum peak intensity of 2292 corresponding to the (6 0 0) reflection plane, indicating a high degree of crystallinity. The indexed powder XRD pattern confirms the formation of a well-ordered crystal structure, as illustrated in Figure 4.

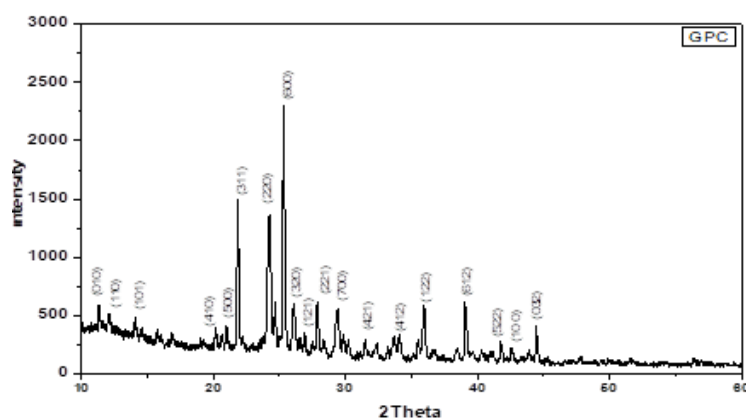


Figure. 4 XRD Spectrum of as grown GPC Crystal

V. NMR Analysis

Nuclear magnetic resonance (NMR) spectroscopy was employed to analyze the molecular structure of the synthesized glycine potassium-calcium nitrate (GPC) crystal and to confirm the presence of functional groups associated with glycine. The ^1H NMR spectrum was recorded using a Mercury Plus Varian spectrometer operating at 300 MHz, while the ^{13}C NMR spectrum was obtained using a Bruker AV-500 spectrometer at a frequency of 500 MHz. The ^1H NMR spectrum displayed characteristic chemical shifts corresponding to the amine ($-\text{NH}_2$) and methylene ($-\text{CH}_2$) protons of glycine. The $-\text{NH}_2$ group appeared at $\delta = 4.671$ ppm, and the $-\text{CH}_2$ protons were observed at $\delta = 3.465$ ppm. In the ^{13}C NMR spectrum, the methylene carbon appeared at $\delta = 41.396$ ppm, while the carboxylate carbon ($-\text{COO}^-$) showed a distinct signal at $\delta = 172.481$ ppm, confirming the presence of glycine in its zwitterionic form. These chemical shifts are in agreement with reported values for glycine-based complexes, validating the molecular integrity and coordination environment in the GPC crystal. The comparative ^1H and ^{13}C chemical shift assignments are summarized in Table 2 [18].

Table 2 ^1H NMR and ^{13}C NMR Chemical Shifts for GPC sample

$^1\text{H-nmr}$		$^{13}\text{C-nmr}$	
$\delta(\text{NH}_2)$ ppm	$\delta(\text{CH}_2)$ ppm	$\delta(\text{COO}^-)$ ppm	$\delta(\text{CH}_2)$ ppm
4.671	3.465	172.481	41.396

VI. FTIR And Raman Analysis

Fourier-transform infrared (FTIR) and Raman spectroscopy were employed to elucidate the vibrational modes and confirm the presence of functional groups in the glycine potassium-calcium nitrate (GPC) crystal. FTIR spectra were recorded in the KBr phase over the spectral range of 400–4000 cm^{-1} using a Perkin Elmer infrared spectrometer (1600 series), with a resolution of 4 cm^{-1} and a scanning speed of 2 mm/s [13,14]. The Raman spectra were obtained in solid phase using a Jobin Yvon Raman spectrometer (HG-2S) with an Ar^+ laser source ($\lambda = 5145 \text{ \AA}$) in the range of 200–3500 cm^{-1} . The FTIR spectrum (Fig. 5) revealed strong absorption peaks primarily in the 400–1600 cm^{-1} region, corresponding to characteristic molecular vibrations. A broad absorption band was observed between 1400–3200 cm^{-1} , attributed to overlapping N–H and O–H stretches. Peaks between 506.9–677.0 cm^{-1} were assigned to carboxylate group vibrations of glycine in its zwitterionic form. Notable features include CH_2 stretching at 2887.5 cm^{-1} , NH_3^+ deformation modes between 1483 and 1632.2 cm^{-1} , and NO_3^- symmetric and asymmetric stretches at 1036.5 cm^{-1} , 1333.2 cm^{-1} , and 1383.8 cm^{-1} .

Raman spectra (Fig. 6) complemented the FTIR data, resolving additional modes that were either weak or absent in the IR spectrum. Lattice vibrations were clearly observed at 104.6 cm^{-1} and 149.4 cm^{-1} , and CH_2 stretching modes were more prominent in Raman, especially at 2949.2 cm^{-1} , 2965.5 cm^{-1} , and 3018.6 cm^{-1} . The NH_3^+ stretching vibrations were also well-resolved in both spectra. The combination of FTIR and Raman spectroscopy provides a detailed vibrational profile of the GPC crystal, confirming its molecular structure and the presence of glycine, nitrate, and metal-ligand coordination. A comparative summary of key IR and Raman vibrational assignments is presented in Table 3.

Table 3 FTIR and Raman assignments.

IR ($\nu \text{ cm}^{-1}$)	Raman ($\nu \text{ cm}^{-1}$)	Assignments
—	104.6	Lattice vibrations
—	149.4	Lattice vibrations
506.9	518.5	COO^- rocking
593.5	584.7	M–N bond
607.8	606.9	COO^- bending
675.0	688.1	COO^- wagging
899.0	894.0	CNN symmetric stretching
934.7	942.5	CH_2 wagging
1036.5	1049.6	NO_3^- symmetric stretch
1122.1	1121.7	NH_3^+ rocking
1158.7	1153.9	NH_3^+ rocking
1332.9	1337.1	CH_2 wagging/twisting
1333.2	1336.2	NO_3^- asymmetric stretch
1383.8	1398.3	NO_3^- asymmetric stretch
1437.1	1462.7	CH_2 scissoring
1483.0	1498.1	NH_3^+ deformation
1530.4	1542.0	NH_3^+ deformation
1596.6	1580.6	NH_3^+ deformation
1632.2	1630.9	NH_3^+ deformation
—	2002.8	Amino acid combination band
2273.9	2229.6	Amino acid combination band
2237.5	2233.1	N–H bonded oscillation
—	2278.9	NH_3^+ stretch

2791.4	2705.7	NH ₃ ⁺ stretch
2887.5	2865.3	NH ₃ ⁺ stretch
—	2949.2	CH ₂ stretching
2962.4	2965.5	CH ₂ stretching
—	3018.6	CH ₂ stretching
3105.8	3096.0	NH ₃ ⁺ stretching

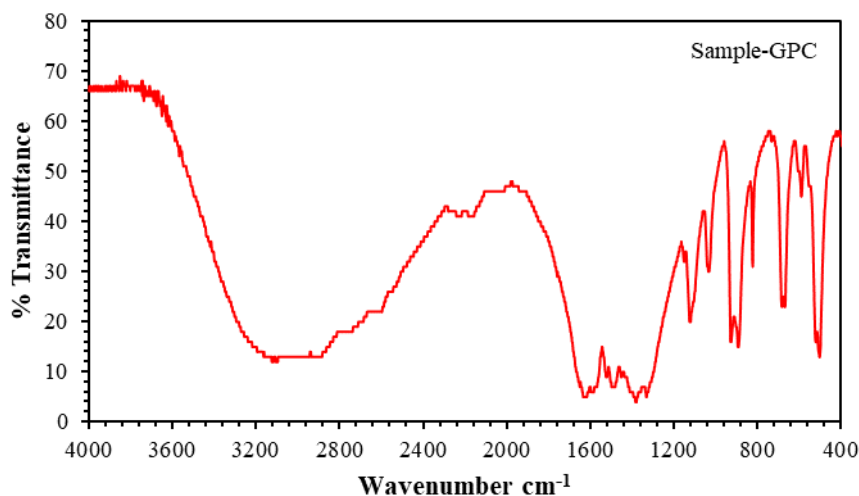


Figure. 5. FTIR spectrum of GPC crystal.

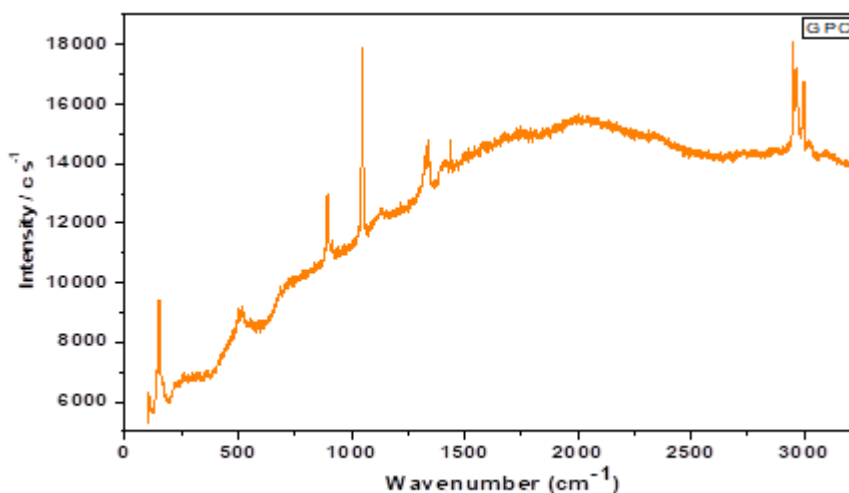


Figure. 6. Raman spectrum of GPC crystal.

VII. UV Analysis

The UV–visible absorption spectrum of the GPC crystal was recorded using a Hitachi spectrophotometer (U-2900) in the wavelength range of 100–1200 nm, covering the entire ultraviolet and near-visible regions [15]. The spectrum revealed a sharp absorption cut-off at 222 nm, which corresponds to an optical band gap energy of 5.59 eV [19]. The GPC crystal exhibits a broad optical transparency window ranging from 300 nm to 1200 nm, encompassing a significant portion of the UV, visible, and near-infrared regions. This wide transparency range is indicative of low optical absorption across these wavelengths, a key requirement for materials intended for nonlinear optical and optoelectronic applications. The combination of a high band gap and excellent optical clarity suggests that GPC is well-suited for applications such as optical windows, photovoltaic devices, frequency converters, and optical sensors. These findings underscore the potential of GPC crystals as functional materials in advanced photonic and optoelectronic technologies, where wide-bandgap materials with high transparency are critical.

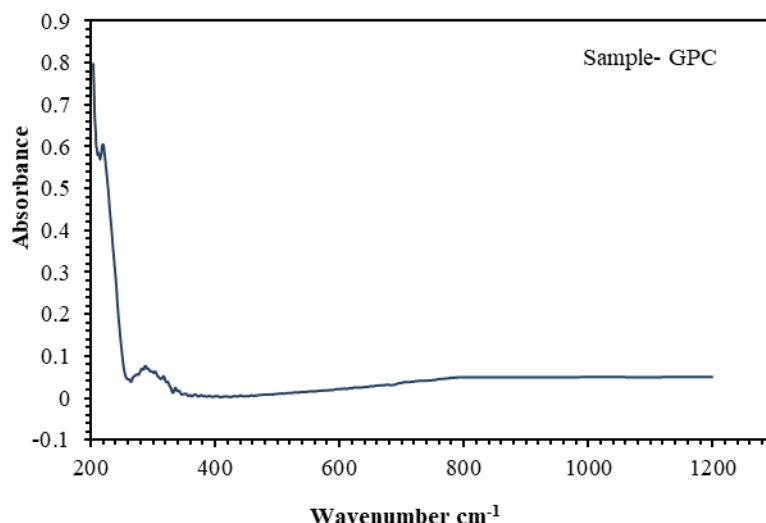


Figure.7. UV–vis-NIR spectrum of GPC crystal.

VIII. Powder SHG Measurement

The second harmonic generation (SHG) efficiency of the synthesized GPC crystal was evaluated using the modified Kurtz and Perry powder technique [16]. For this purpose, a Q-switched Nd:YAG laser operating at a fundamental wavelength of 1064 nm, with a pulse energy of 2.69 mJ/pulse, pulse width of 8 ns, and a repetition rate of 100 Hz, was employed as the excitation source. The GPC crystals were finely ground to a uniform particle size of approximately 125–150 μm and tightly packed between two transparent glass slides. The packed sample was then irradiated by the laser beam, and the generated SHG signal at 532 nm (green light) was detected and displayed on a cathode ray oscilloscope. The SHG output voltage for the GPC crystal was recorded as 85 mV, compared to 185 mV for a standard potassium dihydrogen phosphate (KDP) crystal under identical experimental conditions. This indicates that the SHG efficiency of GPC is approximately 0.45 times that of KDP. It is important to note that SHG efficiency can vary depending on several factors including crystal composition, growth conditions, crystallite size, and packing density during the measurement. Nonetheless, the observed nonlinear response confirms the NLO activity of the GPC material, highlighting its potential for photonic applications.

IX. I–V And Photoconductivity Studies

The current–voltage (I–V) and photoconductivity characteristics of the GPC crystals were investigated using a SCIENTIFIC digital Pico-ammeter (DPM 111). For this analysis, polished single crystals of approximately 4 mm thickness were prepared by applying silver electrodes on opposite faces. These were mounted between two copper electrodes in a parallel plate capacitor configuration to ensure uniform field distribution. The I–V characteristics were recorded by applying a DC voltage in steps from 0 to 30 V, and the corresponding current values were measured both in dark and under illumination. The resulting data were plotted as shown in Figure 8. The current was observed to increase linearly with voltage up to the threshold value of 30 V, indicating ohmic behavior and defining the safe operating range for the material.

Upon exposure to light, a decrease in current was observed compared to the dark current, indicating negative photoconductivity. This phenomenon is characterized by a reduction in the number of free charge carriers under illumination and can be explained by the Stockman model, which attributes the behavior to the trapping of charge carriers or recombination processes induced by photoexcitation [20,21]. The observed negative photoconductivity suggests potential applications of GPC crystals in photosensitive and photonic switching devices, where controlled carrier modulation is essential.

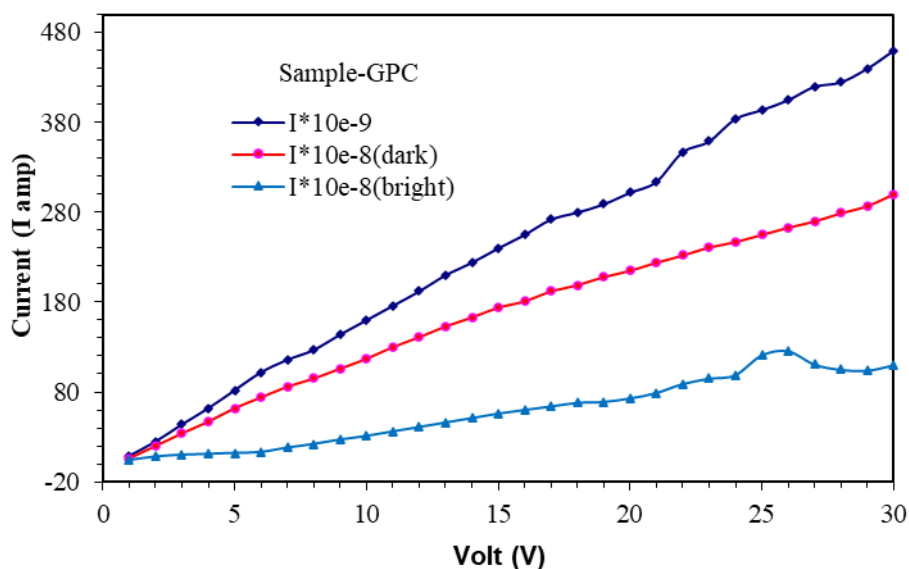


Figure. 8 I–V and Photoconductivity characteristic of GPC crystal.

X. Conclusion

Transparent crystals of acid-mixed glycine–potassium–calcium nitrate (GPC) were successfully synthesized via the slow evaporation technique at room temperature from an aqueous solution. Comprehensive characterization was carried out to evaluate the physical, chemical, optical, and electrical properties of the grown crystals. Solubility studies showed a linear relationship between solubility and temperature within the range of 300 K to 350 K, while density measurements using the flotation method yielded a value of 1.612 g/cm³. Thermal analysis indicated a melting point of 216 °C and decomposition onset at 235 °C, confirming the thermal stability of the material. Elemental analyses using CHN and EDAX verified the expected chemical composition, confirming the integration of both organic (glycine) and inorganic (potassium and calcium nitrate) components in the crystal matrix. The consistency between experimental and theoretical values confirms the purity and reproducibility of the synthesized compound. FTIR and Raman spectroscopic studies revealed the presence of key functional groups and indicated a non-centrosymmetric molecular structure, a critical requirement for second-order nonlinear optical (NLO) applications.

Optical measurements demonstrated a broad transparency window (300–1200 nm) and an optical band gap of 5.59 eV, making GPC suitable for optoelectronic and photonics applications. The SHG efficiency, evaluated using a Q-switched Nd:YAG laser ($\lambda = 1064$ nm), was found to be 0.45 times that of KDP, confirming its moderate yet promising nonlinear optical performance. Electrical characterization revealed an ohmic I–V behavior up to 30 V, while photoconductivity studies showed negative photoconductivity under illumination. This suggests photo-induced charge carrier recombination, consistent with the Stockman model, and highlights the crystal's potential use in light-sensitive and switching devices. Overall, the GPC crystal exhibits a favorable combination of NLO activity, optical transparency, thermal stability, and negative photoconductivity, positioning it as a promising multifunctional material for use in nonlinear optics, optoelectronics, and photoconductive device applications.

Acknowledgment

The authors gratefully acknowledge the support and assistance provided by the staff of the Department of Material Science at Tata Institute of Fundamental Research (TIFR), Mumbai, the Indian Institute of Technology (IIT), Mumbai, the University Institute of Chemical Technology (UICT), Mumbai, and the Materials Research Laboratory, Kaylan. Access to their advanced experimental facilities and equipment was instrumental in the successful completion of this research.

References

- [1] Paredes J.H., Mintik D.G., Negret O.H., Ponce H.E., Alvarez M.E., Mijango R.R., Moller A.D., Journal Of Physics And Chemistry Of Solids, 69(2008), 1974-1981.
- [2] Paredes J.H., Mintik D.G., Negrete O.H., Ponce H.E., Ramos M.E.A., Moller A.D., Journal Of Molecular Structure, 875(2008), 295-301.
- [3] Pepinsky R., Okaya Y., Eastman D.P., Mitsui T., Physical Review, 107(1957), 1538-1544.
- [4] Khandpekar M.M., Pati S.P., Journal Of Optical Communication, 283(2010), 2700-2704.
- [5] Eimert D., Velsko S., Davis L., Wang F., Loiacono G., Kennedy G., IEEE Journal Of Quantum Electronics, 25(1989), 179-184.

- [6] Agarwal M.D., Choi J., Wang W.S., Bhat K., Lal R.B., Shied A.D., Penn B.G., Frazier D.O., *Journal Of Crystal Growth*, 179(1999), 204-209.
- [7] Bhat M.N., Dharmaprakash S.M., *Journal Of Crystal Growth*, 235(2002), 511-516.
- [8] Mohan Rao J.K., Vishwamitra M.A., *Acta Crystallographica*, B28(1972), 1484-1489.
- [9] Natarajan S., *Zeitschrift Für Kristallographie - Crystalline Materials*, 163(1983), 305-306.
- [10] Krishnakumar R.V., Naandhini M.S., Natarajan S., Sivakumar K., Varghese B., *Acta Crystallographica*, C57(2001), 1149-1154.
- [11] Martin Britto S.A., Natarajan S., *Optics Communication*, 281(2008), 457-462.
- [12] Dhanuskodi S., Vasanta K., *Spectrochimica Acta Part A*, 61(2005), 1777-1782.
- [13] Mallik T., Kar T., *Journal Of Crystal Growth*, 274(2005), 251-255.
- [14] Dhanuskodi S., Jeyakumari A.P., Manivannan S., *Journal Of Crystal Growth*, 282(2005), 72-78.
- [15] Manikandan S., Dhanuskodi S., *Spectrochimica Acta Part A*, 67(2007), 197-205.
- [16] Kurtz S.K., Perry T.T., *Journal Of Applied Physics*, 39(1968), 3798-3813.
- [17] Pragasam A.J.A., Mhadavan J., Mohamed M.G., Selvakumar S., Ambujan K., Sagayaraj P., *Optical Materials*, 29(2009), 173-176.
- [18] Silverstein R.M., Bassler G.C., Morrill C., *Spectrometric Identification Of Organic Compounds*, 4th Ed., Wiley, USA, 1991.
- [19] Balakrishnan T., Ramamurthi K., *Crystal Research And Technology*, 12(2006), 1184-1188.
- [20] Dongare S.S., Patil S.B., Khandpekar M.M., *AIP Conference Proceedings*, 2265(2020), 030403(1-3).
- [21] Bube R.H., *Photoconductivity Of Solids*, Wiley, New York, 1981.